Hybrid Force/Stress Control Method for Robotic Polishing System Based on Hertzian Contact Theory

Chuangfeng Huai[1, a *], Gangyi Shi[1,b] Fengfeng(Jeff) Xi[2,c]

[1]School of Mechanical and Vehicle Engineering, East China Jiaotong University, Nanchang, China 330013

[2]Department of Aerospace Engineering, Ryerson Uinversity, Toronto, ON, Canada M5B 2K3

[a]hcf811225@163.com, [b]827036134@qq.com, [c]fengxi@ryerson.ca

Keywords: Robotic polishing; Active compliance; Hybrid torque/stress control; Stress-controlled flange; Constant stress control.

Abstract. At present, high-speed railways have high design speeds and require high surface machining quality. Traditionally, automatic polishing systems are performed using a constant-force adaptive flange, In the face of complex surfaces, especially at the corners, unevenly and excessively polishing occurs. After subsequent spray treatment, problems such as surface ripples and streaks will appear that seriously affect product quality. This paper studies a robotic system that is suitable for polishing complex surface putty layers and develops a force controller to deal with abrupt changes in curvature at the corner of the surface. In order to realize even polishing, a hybrid control strategy based on Hertzian contact theory is proposed. By installing an active compliant device on the robot end-effector, the force control and position control of the tool are decoupled. While the robot controller is used to control the position and orientation of the tool mounted on the robot end-effector, the compliant device controller is used to control the contact force between the tool and the workpiece directly. The simulation results show that the method can track and compensate the target trajectory and realize rapid adjustment of the desired force. The experiment results show that the proposed control method can obtain good surface quality for polishing the vehicle putty layer.

Introduction

With the rapid development of industrial robots, its application in various industrial fields is becoming more and more widespread [1]. Because the robot needs to contact the workpiece during the operation, too big and too small contact force can lead to undesired polishing results. In addition to requiring the position to achieve the required accuracy, the robotic polishing system also required to control the contact force between the robot and the workpiece.

Over the last thirty years or so, a great deal of research has been carried out to develop automated polishing systems and contact force control[2-5]. Mingsheng J [6] proposed based on the robot, the use of airbags to achieve the flexibility of the design of polished control program. By changing their pressure inside the balloon to achieve the adjustment of the polishing contact force, so that the contact force is constant. Nagata F et al. [7] used a position feedback to adjust the force feedback in Cartesian space so that the tool does not deviate from the desired trajectory and the polishing force consisting of contact and dynamic friction can be controlled. Ting Huang et al. [8] proposed a hybrid control strategy by installing a compliant device, one end of the compliant device is mounted at the end of the robot and the other end is connected with the polishing tool. And a constant force control method [9] is proposed to control the contact force between the tool and the workpiece directly. Myers A et al. [10] used the BP neural network PID control strategy to perform polishing contact force control and obtains better processing results. Xudong Zhang et al. [11] introduced the general structure of the constant force polishing end actuator, and designs a set of simple and practical, high control precision and fast response force control algorithm. Constant force polishing process face

complex surfaces, especially at the corners, all of which are unevenly polished and excessively polished. After the subsequent spraying process, water ripples, streaks, etc. will appear, which will seriously affect the product quality. At present, many product lines are artificially modified after machine polishing, and the efficiency is relatively low.

This paper designed a robot end actuator which can adjust the contact force between the polishing tool and the polishing surface according to the different conditions, introduced a hybrid control strategy based on contact theory, the method can realize rapid adjustment of the desired force and realize constant stress contact for process of vehicle putty layer polishing.

1. Contact stress modeling

1.1 Contact area

During the polishing operation, the polishing tool presses against the surface of the part under the action of force/pressure. According to the Hertz theory, an interaction model between the polishing tool and the workpiece to be polished is established [12].

The polishing tool and the surface of part is shown in Figure 1 which is a simple example case in which the part has a semi-elliptical cross-section with a semi-major u=20 cm and a semi-minor axis v=10 cm. The radius of curvature of the part surface changes in one direction and remains constant in the other direction.

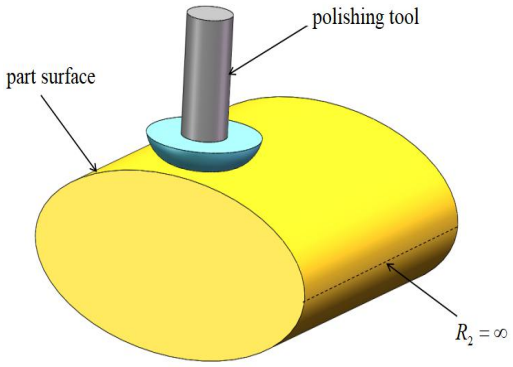

Fig.1 Polishing tool and part

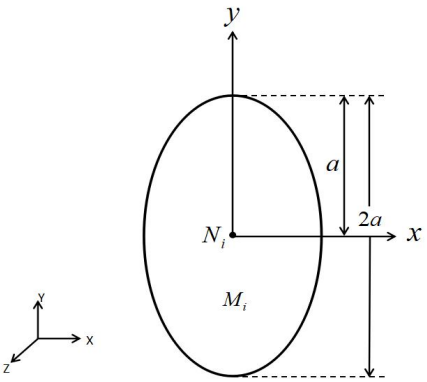

Fig.2 Elliptical contact area

Assume that the polishing tool used is hemispherical, where the polishing tool is tangent to the surface of the part and the centerline is perpendicular to the surface of the part. This implies that the minimum and maximum radius of the polishing tool are equal and, the angle between the principal curvature planes is equal to zero. Therefore, the contact area changes along the part surface. The radius of curvature of the part can be calculated as follows

$$R = uv \Big/ \left(v^2 \cos^2\theta + u^2 \sin^2\theta\right)^{\frac{3}{2}} \tag{1}$$

This equation indicates that for a part with curved profiles the contact area between the polishing tool and the part surface changes with the change in radius of curvature of the part. Contact Area is defined as a two dimensional evidence describing the interaction between the polishing tool and the part surface. Contact Area is a function of the radius of curvature as seen in Figure 2.

The boundary line of the contact surface forms an elliptic area given by

$$x^2/a^2 + y^2/b^2 = 1 \tag{2}$$

a and b are related by $k=b/a$, where b is determined by

$$b = \sqrt[3]{F \frac{3kE(k')}{2\pi} \cdot \Delta} \tag{3}$$

Where, $\Delta = 1/(\alpha+\beta)(\frac{1-\upsilon_1^2}{E_1}+\frac{1-\upsilon_2^2}{E_2})$, υ_1 and υ_2 are the Poisson's ratios of the discs, E_1 and E_2 are the modulus of elasticity of body, the constants α and β depend on the principal radii of curvature of both discs at the point of contact, and $E(k')$ is the complete elliptic integral

$$E(k') = \int_0^{\frac{\pi}{2}} \sqrt{1 - k'^2 \sin^2\theta}\, d\theta \tag{4}$$

1.2 **Constant stress modeling**

Contact stress refers to the pressure arising from two bodies subjected to compressive loading by forcing them together. The principal stress on the contact surface, through simplification for the polishing case, is given as follows[13]

$$\sigma_0 = b/E(k')\Delta \tag{5}$$

In practice, the user specified polishing stress is considered as the mean stress and the stress is highest when the radii are smallest. The mapping of contact stress on the surface radii of curvature proves the applied force cannot remain constant if contact stress is required to be constant. By solving for the force, an equation is obtained for determining the force variation necessary for keeping contact stress σ_0 constant.

$$F = \frac{2\pi E^2(k')\Delta^2 {\sigma_0}^3}{3k} \tag{6}$$

2. Design of the stress controller

2.1 **Contract force based on air cylinder pressure control**

When the constant-stress flange mechanism is working, the gas pressure in the air spring is $\boldsymbol{P_0}$,the force area is A, and the displacement of the air spring under the action of the gas is x which is determined by the displacement sensor, and the constant-stress of flange mechanism and the connection component is M, as shown in Figure 3.

The pressure sensor is located in the electrical proportional valve and is used to real-time detect the pressure in the air spring. Then the contact force $\boldsymbol{F_p}$ is applied to the polishing tool, but in reality, the $\boldsymbol{F_f}$ acts on the workpiece surface also consider the gravity mg of the polishing tool itself, and then the equation is given by

$$M\ddot{x} + C_p\dot{x} + Kx = P_o A - F_p \tag{7}$$

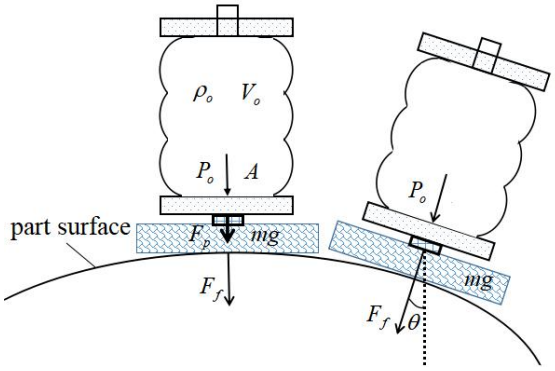

Fig. 3 Force analysis of flange

Where, $F_p = F_f - mg\cos\theta$, M is the tool mass, C and K are the damping and stiffness of the spring inside the cylinder, A is the area of the piston inside the cylinder chamber. Then, Laplace transforms are performed for the simultaneous expressions (7)

$$M_{s^2}X(s) + C_p sX(s) + KX(s) = P_o(s)A - F_P(s) \tag{8}$$

When the polishing tool is in contact with the workpiece surface, the force is F_f. The resulting displacement is shown in Figure 4 as x, and the equivalent stiffness coefficient is K_e, which results in:

$$F_f(s) = K_e X(s) \tag{9}$$

The simultaneous expressions (8) and (9) are:

$$F_f(s) = \frac{P_o(s) K_e A}{Ms^2 + C_p s + K + K_e} \tag{10}$$

The applied force cannot remain constant if contact stress is required to be constant. When the position of the contact point between the polishing tool and the workpiece changes, the radius of curvature of the contact point will change, and the contact area between the polishing tool and the workpiece will also change.

2.2 **Control system**

To achieve uniform polishing of curved workpiece, there are two control inputs, one for the pressure valve and another for the flow valve. There are two outputs, one being the contact stress and another being the tool spindle speed. Combines the advantages of PID controller and fuzzy controller, and controls and optimizes the stress control flange system. According to the set input signal and feedback signal, the error and the current error rate are calculated. The fuzzy rules are used to carry out fuzzy reasoning and pass the PID at the same time. The control is adjusted to combine the output of the two controllers for control of the output signal of the stress control flange as shown in Figure 4.

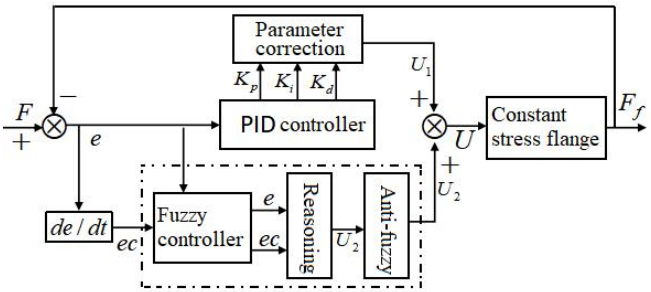

Fig. 4 Close loop control block diagram

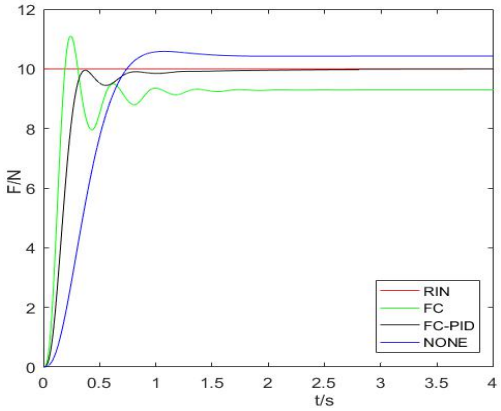

Fig. 5 Force trajectory tracking

In order to verify the control effect of the fuzzy PID controller, experiment of the cylinder force tracking for the polishing control. It can be seen in Figure 5 that under the influence of different control parameters, the error band of line and line is very long and the steady-state error is large, which will cause the transition time to reach steady state to lengthen. Under the fuzzy PID control, although the system response time is later than the pure fuzzy control, the steady-state error of the system is eliminated, the overshoot is basically not occurred, and it quickly reaches the steady state and reaches the set expected value. That means the measured cylinder force follows the planned cylinder force by using the fuzzy PID controller.

3. Robotic polishing Control

3.1 **Modeling of polishing system**

As shown in Figure 6, P is the sampling point on the surface of the ellipsoidal polishing path, (x_p, z_p) is the corresponding coordinate of the P point in the plane X-Z, d is the polishing thickness, and θ is the angle between the axis z and the polishing tool. In order to simplify the

calculation process without affecting the calculation result, it is assumed that the two minor axes of the ellipsoid are the same, that is, the surface equation of the workpiece to be polished is set as:

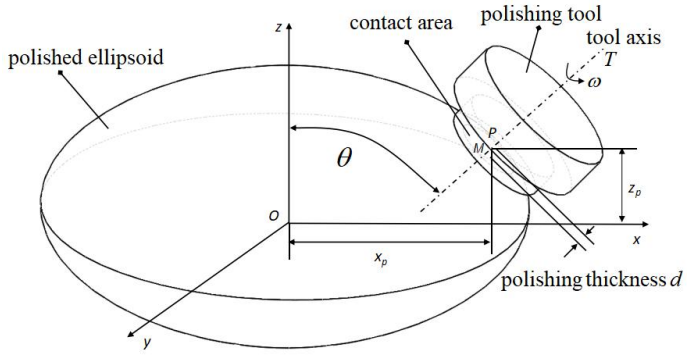

Fig.6 Geometric sketch of polishing

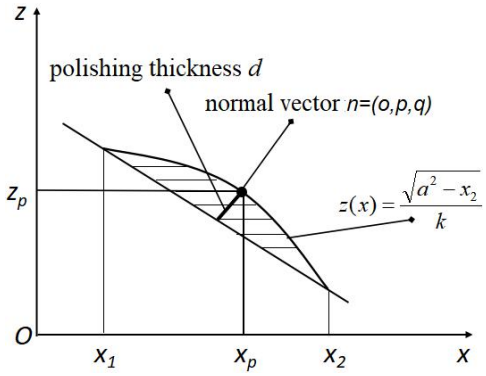

Fig.7 Analysis of cross section

$$F(x,y,z)=\frac{x^2}{100^2}+\frac{y^2+z^2}{50^2}-1=0(0\le z\le 50mm) \tag{11}$$

The cross section equation is

$$z=-\frac{x_p}{k\sqrt{a^2-x_p^2}}\left[x-\left(x_p-\frac{x_p d}{\sqrt{x_p^2+k^4z_p^2}}\right)\right]+\left(z_p-\frac{k^2z_p d}{\sqrt{x_p^2+k^4z_p^2}}\right) \tag{12}$$

The ellipsoid section curve equation in Figure 7 is

$$z=\sqrt{a^2-x^2}\big/k \tag{13}$$

In combination equation (12) and (13), the chord length in the plane is

$$l=\frac{|x_2-x_1|}{\cos\theta}=\left|\frac{2\sqrt{a^4-(a^2-d\sqrt{(1-k^2)x_p^2+a^2k^2})^2}\sqrt{a^2-x_p^2}}{a^2\cos\left(\arctan\dfrac{-x_p}{k\sqrt{a^2-x_p^2}}\right)}\right| \tag{14}$$

The cross-sectional area of contact area between polishing tool and ellipsoid is

$$A=\frac{\pi d^2}{8}=F(d,x_p)=\frac{\pi(a^2-x_p^2)\left[a^4-(a^2-d\sqrt{(1-k^2)x_p^2+a^2k^2})^2\right]}{2\left[a^2\cos\left(\arctan\dfrac{-x_p}{k\sqrt{a^2-x_p^2}}\right)\right]^2} \tag{15}$$

The expression for polishing thickness d is

$$d=F^{-1}(A,x_p)=\frac{a^2-\sqrt{a^4-\dfrac{2A\left[a^2\cos\left(\arctan\dfrac{-x_p}{k\sqrt{a^2-x_p^2}}\right)\right]^2}{\pi(a^2-x_p^2)}}}{\sqrt{(1-k^2)x_p^2+a^2k^2}} \tag{16}$$

P is the sampling point on the surface of the ellipsoidal surface, and M is any point on the contact area, and the velocity at point M is

$$\vec{v} = \vec{\omega} \times \vec{r} \tag{22}$$

Where, r is the distance vector from P to M.

$$\vec{r} = (x - x_p) \cdot \vec{i} + (y - y_p) \cdot \vec{j} + (z - z_p) \cdot \vec{k} \tag{23}$$

$\vec{\omega}$ is the angular velocity of M point rotation about axis $\vec{T}$, then ω can be expressed as

$$\vec{\omega} = \omega \cdot \vec{T} \Big/ \left|\vec{T}\right| \tag{24}$$

The linear equation of axis $\vec{T}$ is

$$(x - x_p) \Big/ o = (y - y_p) \Big/ p = (z - z_p) \Big/ q \tag{25}$$

Where, (o, p, q) is the normal vector perpendicular to the contact surface, that is, the first-order partial derivative of the ellipsoidal equation $F(x, y, z)$, is expressed as

$$o = \frac{\partial F(x,y,z)}{\partial x}; p = \frac{\partial F(x,y,z)}{\partial y}; q = \frac{\partial F(x,y,z)}{\partial z} (x = x_p, y = 0, z = z_p) \tag{26}$$

Then, the expression for $\vec{T}$ is

$$\vec{T} = o \cdot \vec{i} + p \cdot \vec{j} + q \cdot \vec{k} \tag{27}$$

According to Equation (22) and (25), $\vec{\omega}$ can be expressed as

$$\vec{\omega} = \frac{x_p p \omega}{\sqrt{b^4 x_p^2 + a^4 z_p^2}} \cdot \vec{i} + \frac{z_p p \omega}{\sqrt{b^4 x_p^2 + a^4 z_p^2}} \cdot \vec{j} \tag{28}$$

Get the velocity expression at point M is

$$\vec{v} = \frac{z_p a^2 \omega y}{\sqrt{b^4 x_p^2 + a^4 z_p^2}} \cdot \vec{i} + \frac{x_p b^2 \omega (z - z_o) - z_p a^2 \omega (x - x_p)}{\sqrt{b^4 x_p^2 + a^4 z_p^2}} \vec{j} + \frac{z_p b^2 \omega y}{\sqrt{b^4 x_p^2 + a^4 z_p^2}} \vec{k} \tag{29}$$

According to the Equation (29), the velocity distribution at any point M can be found. Under the action of constant stress, the lowest point where the curvature of the workpiece is the largest, and the polishing speed here is close to 0. The polishing speed of the point on contact area becomes smaller with the sampling point of abscissa increases. That is to say, during the polishing operation, in the position where the ellipsoidal curvature is relatively large, in order to ensure the consistency of the entire workpiece polishing effect, as the polishing contact area becomes smaller, the polishing speed of the polishing tool is reduced correspondingly during grinding. The contact force and the polishing speed are related to the polishing point of the ellipsoid.

3.2 **Experimental test**

As shown in Figure 8, the automatic polishing system performs polishing tests on the curved door baffles using constant contact force and constant contact stress, respectively. This test is a fixed position test and does not require position adjustment. During the polishing process, the contour of the part was measured using a 2-D laser profile scanner with an accuracy of 10 microns and a dynamic resolution of 1.0 microns. For constant force grinding, the cylinder pressure remains constant at 2.25 bars. For the constant contact stress grinding, the polishing speed and the contact force are determined according to the curvature of different coordinate positions. Using the parameter planning method, the cylinder pressure is from 1.71 to 2.30 bars. The pressure range is based on the required 50 N/mm2 contact stress. When the polishing tool reaches the top of the polishing arc, 2.30 bar is required, while the arcuate end edge requires

1.71 bar.

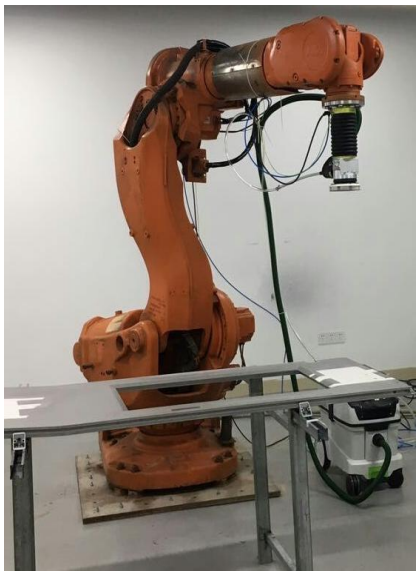

Fig.8 Automatic polishing system

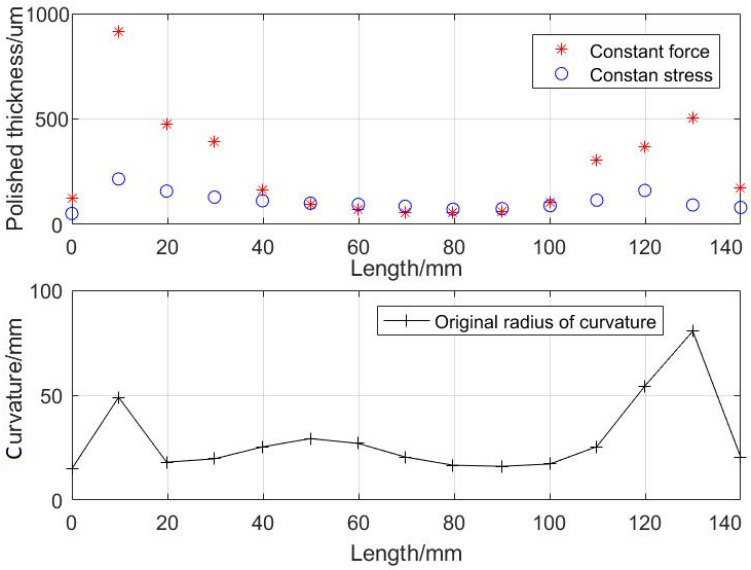

Fig.9 Result between constant force and constant contact stress

Figure 9 shows the experiment result performed on the polished thickness at different curvature radius positions for the curved door baffle. Near the middle of the part the radius of curvature is large, the constant force produced a similar polished thickness to that by the constant stress, and both very close the original Ideal value. However, at both ends where the radius of curvatures become small, the constant force case removed more materials due to high concentrated force. For the constant contact stress case, the polished thickness is still very close to the original Ideal value, the polishing effect can be better realized and expected.

4. Conclusion

This paper proposed a stress control method for automatic polishing system based on Hertz contact theory. By installing an active air spring device at the end of the robot, the output force of the device can be controlled by controlling the air pressure in the cylinder chamber. Therefore, the contact force of the workpiece processing is controlled in accordance with the contact area and the desired constant contact stress. The theoretical model of the constant stress control device was deduced and the force control strategy was analyzed. The position control of the system is completed by the robot controller. The active air spring device provides feedback of the end displacement deviation to the robot controller. Based on the size of the deviation, it is judged whether the posture compensation is required. The experimental results show that this kind of constant stress control method responds quickly to disturbance regulation. By polishing the curved door panel, the polishing effect can be basically the same for the plane and the curved surface, and the system has good polishing uniformity.

Acknowledgments

This paper is supported by DEF of Jiangxi (GJJ150493), NSF of Jiangxi (20151BBE50117) and NSF of China (51675180).

References

[1] Wang Tianmiao, Tao Yong, Research status and industrialization development strategy of Chinese industrial robot, Journal of Mechanical Engineering, 9 (2014) 1-13. (in Chinese).

[2] Pessoles, X., and Tournier, C. Automatic Polishing Process of Plastic Injection Molds on a 5-axis Milling Center, Journal of Materials Processing Technology, 209 (2009) 3665-3673.
[3] M. J. Tsai, Jou-Lung Chang, Jian-Feng Haung, Development of an automatic mold polishing system, IEEE Transactions on Automation Science and Engineering, 4(2005): 393-397.
[4] Yuta Oba, Yuki Yamada, Yasuhiro Kakinuma, Simultaneous Control of Tool Posture and Polishing Force on Unknown Curved Surface for Serial-Parallel Mechanism Polishing Machine[C]//IEEE Conference of the Industrial Electronics Society, Yokohama, IEEE, 2016: 5351-5356.
[5] Fengfeng(Jeff) Xi, Tianyan Chen, Shuai Guo, Robotic Polishing and Deburring, in: Hashmi, M.S.J. (Eds.), Comprehensive Materials Finishing. Oxford: Elsevier, 2017, pp. 121-153.
[6] Mingsheng Jin. "Research on the free surface of mould gasbag polishing mechanism and process," Zhejiang: Zhejiang University of Technology, 2009. (in Chinese)
[7] Nagata F, Watanabe K, Kusumoto Y, Generation of normalized tool vector from 3-axis CL data and its application to a mold polishing robot[C]//IEEE International Conference on Intelligent Robots and Systems. IEEE, 2004: 3971-3976 vol.4.
[8] Ting Huang, Chuang Li, Zhenhua Wang, Lining Sun, Guodong Chen, Design of a Flexible Polishing Force Control Flange[C]//IEEE International Workshop on Advanced Robotics and its Social Impacts. IEEE, 2016: 91-95.
[9] Ting Huang, Chuang Li, Zhenhua Wang, Yiming Liu, Guodong Chen, A Flexible System of Complex Surface Polishing based on the Analysis of the Contact Force and Path Research[C]//IEEE International Workshop on Advanced Robotics and its Social Impacts. IEEE, 2016: 289-293.
[10] Myers A, Teo C L, Fermuller C, et al. Affordance detection of tool parts from geometric features[C]//IEEE International Conference on Robotics and Automation. Piscataway, USA: IEEE, 2015: 1374-1381.
[11] Xudong Zhang, Hao chen, Ning Yang, A Structure and Control Design of Constant Force Polishing End Actuator Based on Polishing Robot[C]//IEEE International Conference on Information and Automation, Macau SAR, China: IEEE, 2017: 764-768.
[12] Roswell, A. Modelling for Contact Stress Control in Automated Polishing, Master of Applied Science Thesis, Ryerson University, 2004.
[13] Liao, L, Xi, F., and Liu, K., Modeling and Control of Automated Polishing/Deburring Process Using a Dual-purpose Compliance Toolhead, International Journal of Machine Tools & Manufacture, Vol. 48 No.12-13, pp. 1454-1463, 2008.